PicoQuant

Crossing the Border Towards Deep UV – Time-resolved Microscopy of Native Fluorophores

Sandra Orthaus[1], Volker Buschmann[1], Marcelle König[1], Sebastian Tannert[1], Thomas Schönau[1], Reinhild Beyreiss[2], Stefan Nagl[2], Detlev Belder[2], Rainer Erdmann[1]

[1] PicoQuant GmbH, Rudower Chausse 29, 12489 Berlin, Germany, www.picoquant.com
[2] University Leipzig, Institute of Analytical Chemistry, Linnéstr. 3, 04103 Leipzig, Germany

Motivation

Confocal microscopy allows for various fluorescence applications that have found their way into modern biology and medicine leading to new insights into morphology, physiology as well as pathological alterations. Common microscopical analyses include labeling of the sample with extrinsic fluorophores since DNA, saccharides, lipids, membranes, and most cellular structures are non-fluorescent.

To image cellular structures or change spectral properties of the sample one uses extrinsic fluorophores as fluorescence proteins, Quantum Dots, or organic dyes like fluorescein fused to antibodies. However, the labeling strategies as well as fixation and staining might lead to artefacts and thus require careful control experiments to ensure correct localization and functionality of the analyzed system. For example, the expression of fusion proteins containing the green fluorescent protein (GFP) or its derivatives within cells may interfere with the attached protein function due to the relatively larger size of GFP.

To circumvent some of these drawbacks it is desirable to image endogeneous proteins without any labeling. Indeed, a lot of molecules, ranging from small aromatics to large biomolecules, can be detected by their intrinsic fluorescence[1] in the deep UV as they contain appropriate chromophoric groups. Proteins are accessible for deep UV laser-induced fluorescence detection in their native form as
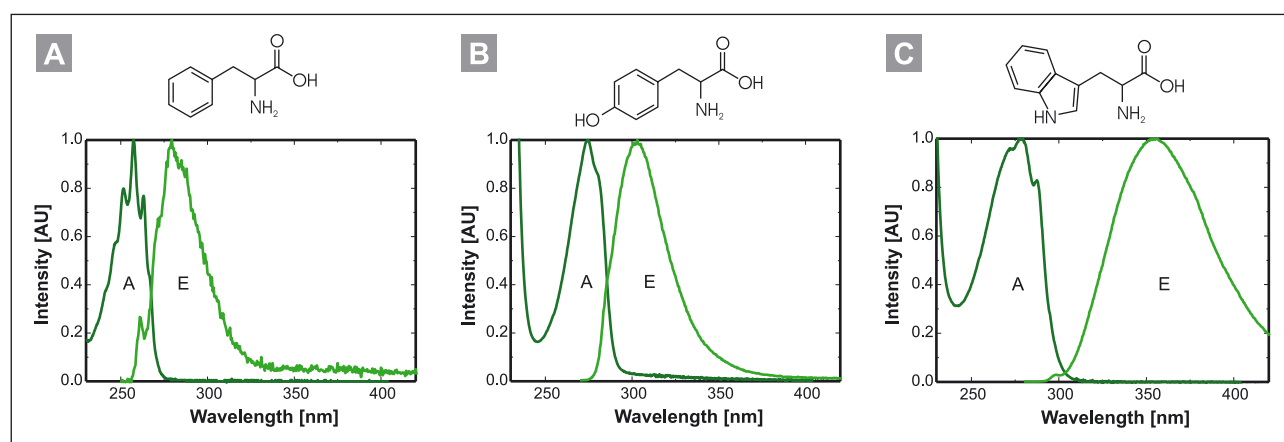

Figure 1: Absorption (A) and emission (E) spectra of the aromatic amino acids Tryptophan (Trp), Tyrosine (Tyr), and Phenylalanine (Phe) in water, 0.1 M phosphate buffer, pH 7. The maxima of Trp excitation and emission are at 295 nm and 353 nm, respectively. The mean fluorescence liftime of Trp is 3.1 ns (in water at pH7). Tyr excitation and emission have their maxima at 275 nm and 304 nm, respectively. Tyr mean fluorescence lifetime is 3.6 ns (in water at pH7). The excitation and emission maxima of Phe are at 260 nm and 282 nm, respectively. Phe has a mean fluorescence lifetime of 6.8 ns (in water at pH7). Data were taken from http://omlc.ogi.edu.

they include the fluorophores tryptophan, tyrosine, and phenylalanine (Figure 1). However, these three aromatic amino acids are relatively rare in proteins and contribute to their UV fluorescence to different degrees. The amount of UV absorbance depends on the number of all aromatic amino acids within the protein. Tryptophan, the largest of the amino acids, is the main contributor and absorbs most of the ultraviolet light compared to tyrosine and phenylalanine. Tryptophan is commonly used to study protein structure, folding and function because its emission is highly sensitive to its local environment. The extinction of tyrosine is much lower and its emission in native proteins is often quenched, e.g., by energy transfer to tryptophan. Due to the low quantum yield of phenylalanine its emission can only be detected in proteins lacking both tryptophan and tyrosine.

More than 20 years ago, single photon counting based techniques evolved as one recognized standard in fluorescence detection. In combination with confocal microscopy FLIM (Fluorescence Lifetime Imaging Microscopy) and FCS (Fluorescence Correlation Spectroscopy) became established techniques for investigations down to the single molecule level. For these applications, PicoQuant provides the time-resolved fluorescence microscope MicroTime 200 as well as FLIM & FCS Upgrade Kits for all major laser scanning microscopes based on the technique of time-correlated single photon counting (TCSPC).

FLIM is a fluorescence imaging technique where the contrast is based on the lifetime of individual fluorophores rather than their emission spectra. The fluorescence lifetime is defined as the average time that a molecule remains in an excited state prior to returning to the ground state by emitting a photon. The lifetime information is used, e.g., for differentiation of fluorophores, to discriminate analyte fluorescence from background noise, to determine local environment conditions (e.g., pH) or ion concentrations, and to study protein interactions via FRET (Foerster Resonance Energy Transfer).

FCS uses the temporal resolution to monitor the characteristic fluorescence intensity fluctuations of particles that diffuse randomly through the confocal observation volume. This technique is applied to measure molecular concentrations, to investigate lateral and rotational diffusion of molecules, their conformational dynamics, the stoichiometry of complex molecules as well as molecular association and dissociation, enzyme dynamics, and intramolecular dynamics in solution on the single molecule level.

Up to date, these experiments typically are carried out in the visible up to the near infrared spectral region. Based on recent advances in fiber amplified laser technology[2] and ultrasensitive detection, we present a novel approach to extend TCSPC into the deep UV using 266 nm excitation. Hereby, direct access is granted to the native fluorescence of biomolecules originating from appropriate chromophoric groups.

Technical Realization

Confocal microscopy with deep UV fluorescence for FLIM and FCS measurements was accomplished using the single molecule sensitive microscope system MicroTime 200. The set-up was modified along the optical path to enable fluorescence excitation at 266 nm and detection in the UV spectral region (Figure 2). As a prerequisite for the implementation of deep UV, the MicroTime 200 was equipped with high-resolution piezo scanning that can be employed in two scanner configurations: object or objective scanning. For image acquisition the objective scanning mode was used, thereby avoiding the problem that mirrors used in typical beam scanning systems like galvo scanners are not suitable for deep UV applications since they do not reflect within this wavelength range. The resulting slower scan speed in the range of a few hundred µs to ms pixel time is not disadvantageous, as this time is anyway needed to collect enough photons per pixel for a decent fluorescence lifetime analysis.

For fluorescence excitation, a 266 nm picosecond pulsed laser (LDH-P-FA 266) was incorporated into the system along with suitable optics and electronics allowing to record photon timing in the UV in the picosecond domain. The picosecond pulsed laser diode head is based on a Master Oscillator Fiber Amplifier (MOFA) concept with optional frequency conversion (Figure 3A). The master oscillator generates infrared picosecond pulses with variable repetition rates up to 80 MHz using the proven gain-switching techniques from PicoQuant. The output of this seed laser is directly connected to a single or double stage fiber amplifier, which boosts the output from the seed laser by several dB while maintaining the other characteristics of the seed laser beam like, e.g., the emission wavelength, polarization, and the short pulse width. The high pulse energies of the amplified infrared lasers permit an efficient wavelength conversion using, for example, single pass second harmonic generation (SHG) or even fourth harmonic generation (FHG). In that way it is for the first time possible to generate picosecond pulses at 266 nm with freely adjustable repetition rates from 1 MHz up to 80 MHz and pulse widths below 100 ps (FWHM, Figure 3B). The laser repetition rate and output power was controlled by the multichannel picosecond pulsed diode laser driver PDL 828 "Sepia II". The overlay of the 266 nm laser with other VIS lasers in the system allows for parallel UV and VIS excitation and enables the analysis of numerous naturally occurring dyes over the spectrum.

All optics required for confocal excitation, beam/focus diagnostics and confocal detection were installed together with the detectors in the self-contained main optical unit (MOU). The optical path within the MOU was modified with quartz optics to enable parallel VIS and UV detection. These alterations included a high-end glycerine immersion
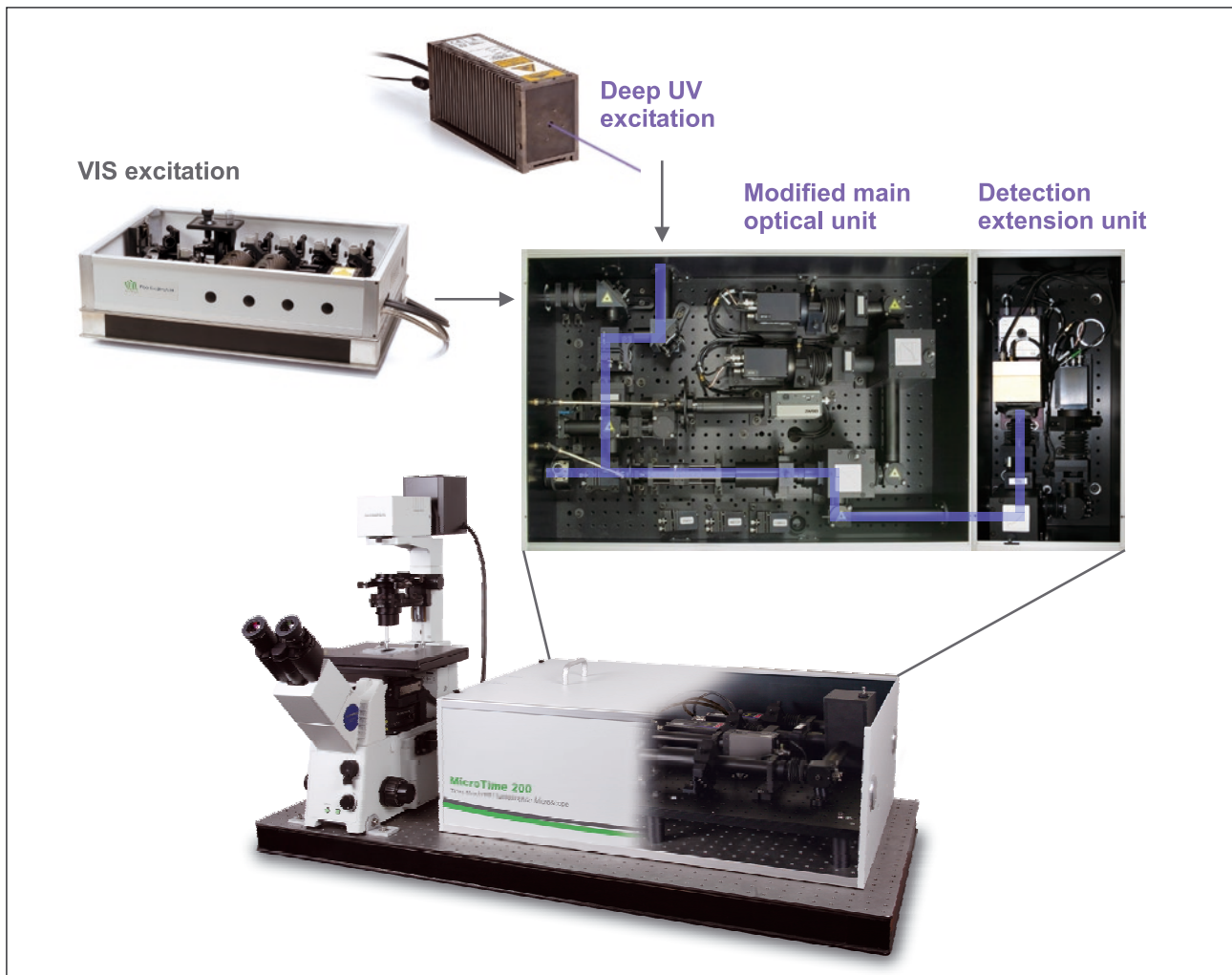
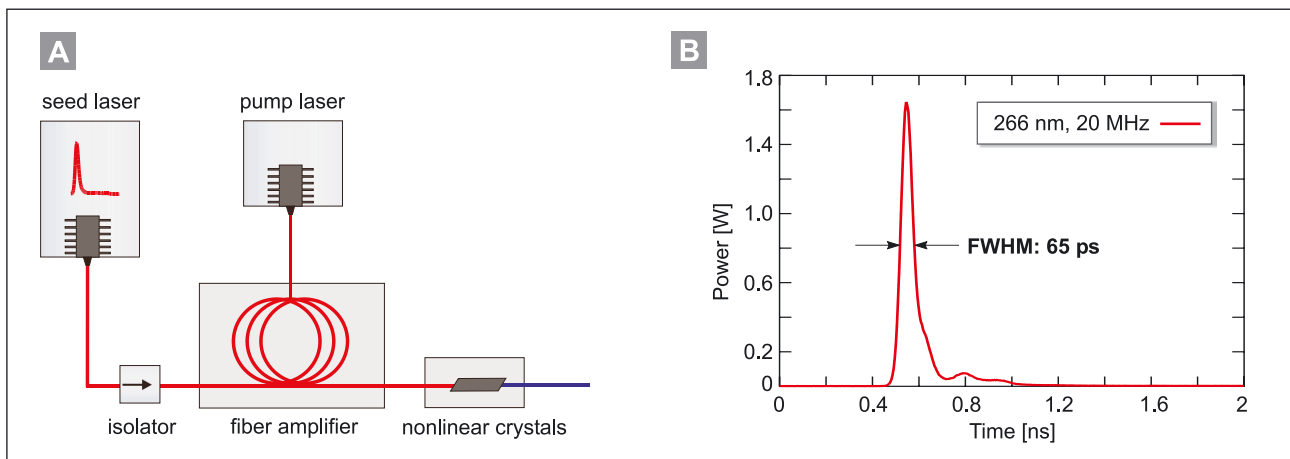*Figure 2: UV MicroTime 200 set-up (for details see text).*

Figure 3: UV 266 nm laser LDH-P-FA 266 (PicoQuant). (A) Scheme of the LDH-FA Series. An infrared picosecond pulsed diode laser acts as a seed laser for a fiber amplifier. The amplified output can then be converted to e.g. UV picosecond pulses. The laser head emits a collimated beam. (B) Pulse shape of the 266 nm laser measured at 20 MHz. The pulse shape remains similar between 1 and 80 MHz and is well below 80 ps.

quartz objective as well as a quartz tube lens. The emitted light was sent through UV lenses and an exchangable confocal pinhole to an ultrabialkali photon counting photomultiplier tube (PMA 165-N-M) synchronized to the laser frequency. This detector offers a detection efficiency of 42 % at 350 nm matching the fluorescence maximum of, e.g., tryptophan.

The fluorescence data were collected by the TCSPC module PicoHarp 300 and have been saved in the unique Time-Tagged Time-Resolved (TTTR)
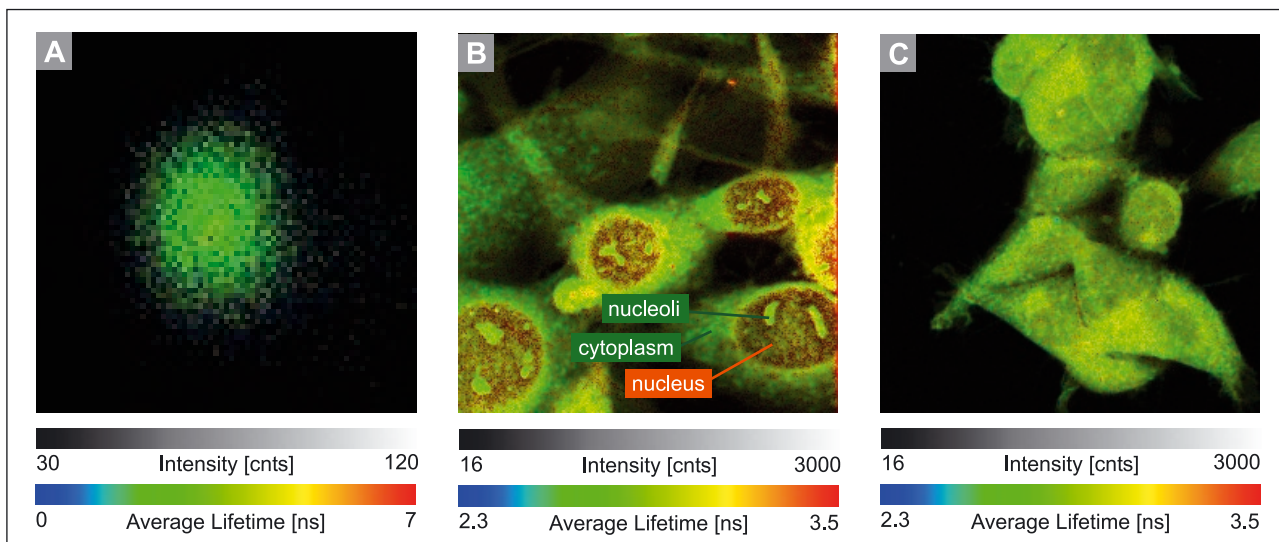
Figure 4: Label-free UV-FLIM. (A) streptavidin-coated beads (Ø 500 nm), immobilized on quartz coverslips, image size 1.5 x 1.5 µm. (B) Mouse 3T3-L1 cells, fixed (methanol), image size 80 x 80 µm. (C) Human HEK293 cells, fixed (paraformaldehyde), image size 73 x 79 µm. Excitation at 266 nm with 20 MHz repetition rate and a pulse width < 100 ps (LDH-P-FA-266, PicoQuant). Quartz objective 40x, NA 0.6, glycerine. Optical filters Z266RDC, longpass 300 nm. Detection with ultrabialkali PMT (42% at 350 nm). (B and C) Sample courtesy of Astrid Tannert, University of Leipzig, Germany.

file format. Data analysis was performed using the SymPhoTime 64 software.

The specially modified UV MicroTime 200 system allows for label-free TCSPC measurements of numerous molecules, ranging from small aromatics to large biomolecules like proteins, by their intrinsic fluorescence.

Results

The new MicroTime 200 set-up enabled us to acquire first results for FLIM and FCS in the deep UV spectral region.

UV FLIM
As a first proof of principle we show Fluorescence Lifetime Imaging (FLIM) with streptavidin coated beads (diameter 540 nm). Streptavidin is a 60 kDa protein that contains 24 tryptophan residues per molecule. The beads were immobilized on a quartz coverslip and were imaged with 266 nm picosecond pulsed excitation (Figure 4A). These beads are suited for determining the optical resolution of the microscope system and, in addition, are often used in binding assays. The single beads on the surface demonstrate the capability of label-free FLIM and show the potential of the instrument for the detection of intrinsic fluorescence of proteins.

Furthermore, we present label-free FLIM of biological cells where the aromatic amino acids (mainly tryptophans) within the proteins become visible (Figure 4B and C). Mouse 3T3-L1 fibroblasts and human HEK293 cells were fixed with methanol and

paraformaldehyde, respectively. In the images, the nucleus is clearly distinguished from the cytoplasm due to the significant shorter fluorescence lifetime. In proteins, the fluorescence lifetime of tryptophan residues typically ranges from 1 to 6 ns, since tryptophan fluorescence is quenched as a result of several phenomena, including binding of ligands, protein-protein association, and protein unfolding. Thus, the presence of multiple tryptophan residues in proteins, each in a different environment, is one reason for the varying fluorescence lifetimes[3]. Inside the nucleus, only the nucleolus is well recognized and shows a similar lifetime as the cytoplasm, illustrating the high protein content within this nuclear region (see Figure 4B). In addition to the aromatic amino acids as protein constituents, other naturally occuring intrinsic fluorophores are found in intact tissues, such as NADH, flavins, collagen, elastin, lipo-pigments, derivatives of pyridol, and porphyrins. A significant fluorescence contribution is due to NADH and flavins, which are excited more specifically at 350 nm. With deep UV excitation, the emission is not due to a single molecular species, but represents all the emitting structures present in a particular cell.

UV FCS
FCS in the deep UV was so far mainly unexplored although this method would allow for numerous analyses of naturally occurring dyes in the UV spectrum. With PMT detectors reaching up to 40 % detection efficiency in the UV, and with high quality objectives suitable for this wavelength range, a path has opened to apply a modern confocal technique like FCS also in the deep UV. The low molecular absorption of aromatic amino acids like tryptophan compared to synthetic fluorophores can be overcome
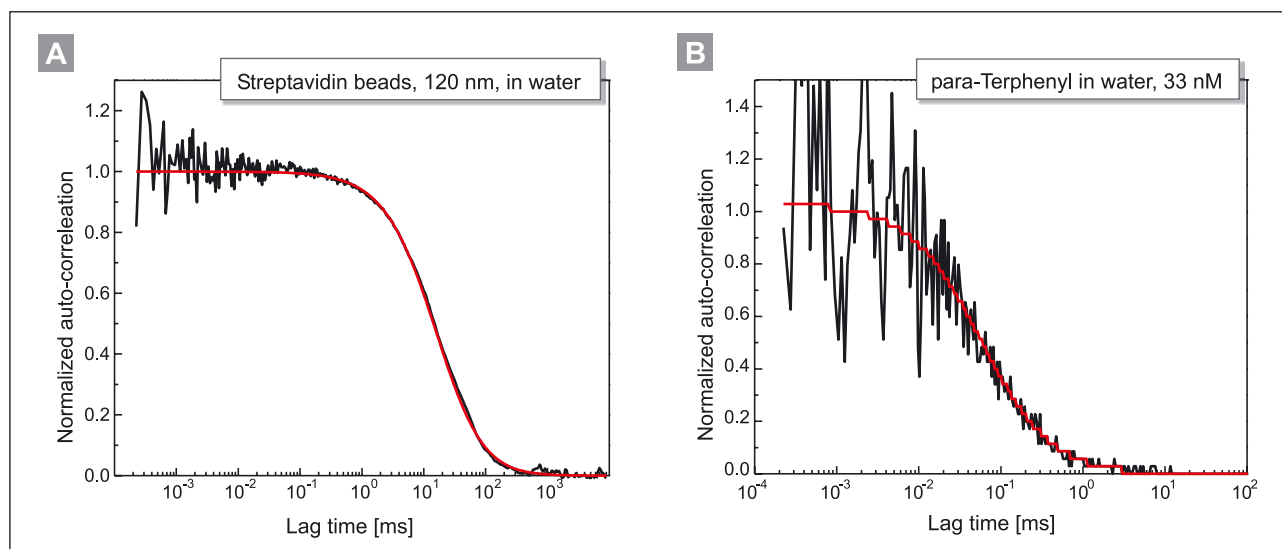
Figure 5: Label-free UV-FCS. (A) Streptavidin-coated beads (Ø 120 nm). Diffusion time t(diff) = 16 ms. Molecular brightness: 1.2 kHz per bead. Laser power approx. 200 µW, 5 min data acquisition. (B) para-Terphenyl. Diffusion time t(diff) = 57 µs. Molecular brightness 510 Hz per molecule. Laser power approx. 220 µW, 10 min data acquisition. Excitation at 266 nm with 20 MHz repetition rate and a pulse width <100 ps (LDH-P-FA-266, PicoQuant). Quartz objective 40x, NA 0.6, glycerine. Optical filters Z266RDC, longpass 300 nm. Detection with ultrabialkali PMT (42 % at 350 nm).

by using streptavidin loaded fluorescent beads with about 120 nm diameter for FCS (Figure 5A). As each bead is labeled with multiple fluorophores, the FCS curve was fitted with a simple diffusion model.

Several other factors are limiting to FCS in the deep UV. In this spectral region almost every material shows absoption and fluorescence. Considering that quarz optics are usually not as transmissive compared to high-end glass devices and that objectives are not available with such high numerical apertures as for the classical water immersion optics, UV FCS is not expected to yield as high molecular brightness values as in the visible range. Furthermore, the sensitivity of PMT detectors is typically not sufficient for this single molecule application which is enhanced by the fact that quantum yield and extinction coefficient of UV dyes are comparatively low. Thus, UV FCS measurements on single chromophores remain a challenging task. Exact buffer preparation is one extremely important factor, as usually any buffer impurities contribute to the background signal.

As a cutting-edge experiment, FCS with laser dyes has been tested using deep UV excitation (Figure 5B). The monomeric organic fluorophore para-Terphenyl with high quantum efficiency in the UV has an absorption coefficient of 33,800cm-1/M at 276.2 nm, a quantum yield of 0.93 and a fluorescence lifetime of 1.21 ns. Using ~220 µW excitation power at a repetition rate of 20 MHz, the diffusion time of para-Terphenyl was significantly shorter than the diffusion time of the much larger streptavidin-coated beads (57 µs vs. 16 ms). For para-Terphenyl a maximum molecular brightness of 570 Hz/molecule was observed.

With these experiments, the optimized MicroTime 200 was shown to be sensitive enough for label-free FCS application. However, while UV FCS has been demonstrated to work, it is not generally applicable for a day to day routine as it strongly depends on sample properties and experimental conditions.

Native analyte identification in microchip electrophoresis by using deep UV fluorescence lifetime measurements

Another application of time-resolved fluorescence microscopy in the deep UV includes microfluidics that can be combined with native analyte fluorescence detection. This approach enables label-free identification of various aromatic analytes and proteins in chip electrophoresis by exciting them in the deep UV spectral region[4].

For this application, the sample was injected into a shorter channel of a fluidic microchip crossing a longer one employed for electrophoresis. Substances were separated in the electric field according to their different molecular size and detected with the confocal microscope set-up MicroTime 200 at 266 nm excitation (Cougar, Time-Bandwidth), (Figure 6A). Fluorescence decay curves were gathered on-the-fly and average lifetimes were determined for the substances in the electropherogram with the aim to identify aromatic compounds in mixtures. Based on TCSPC the background fluorescence has been discriminated resulting in improved signal-to-noise ratios.

Electrophoretic separation was performed with a mixture of small aromatics including serotonin, propranolol, 3-phenoxy-1,2-propanediol, and tryptophan. Figure 6B displays the electropherogram of the four separated compounds and the fluorescence decay curves that could be constructed for each
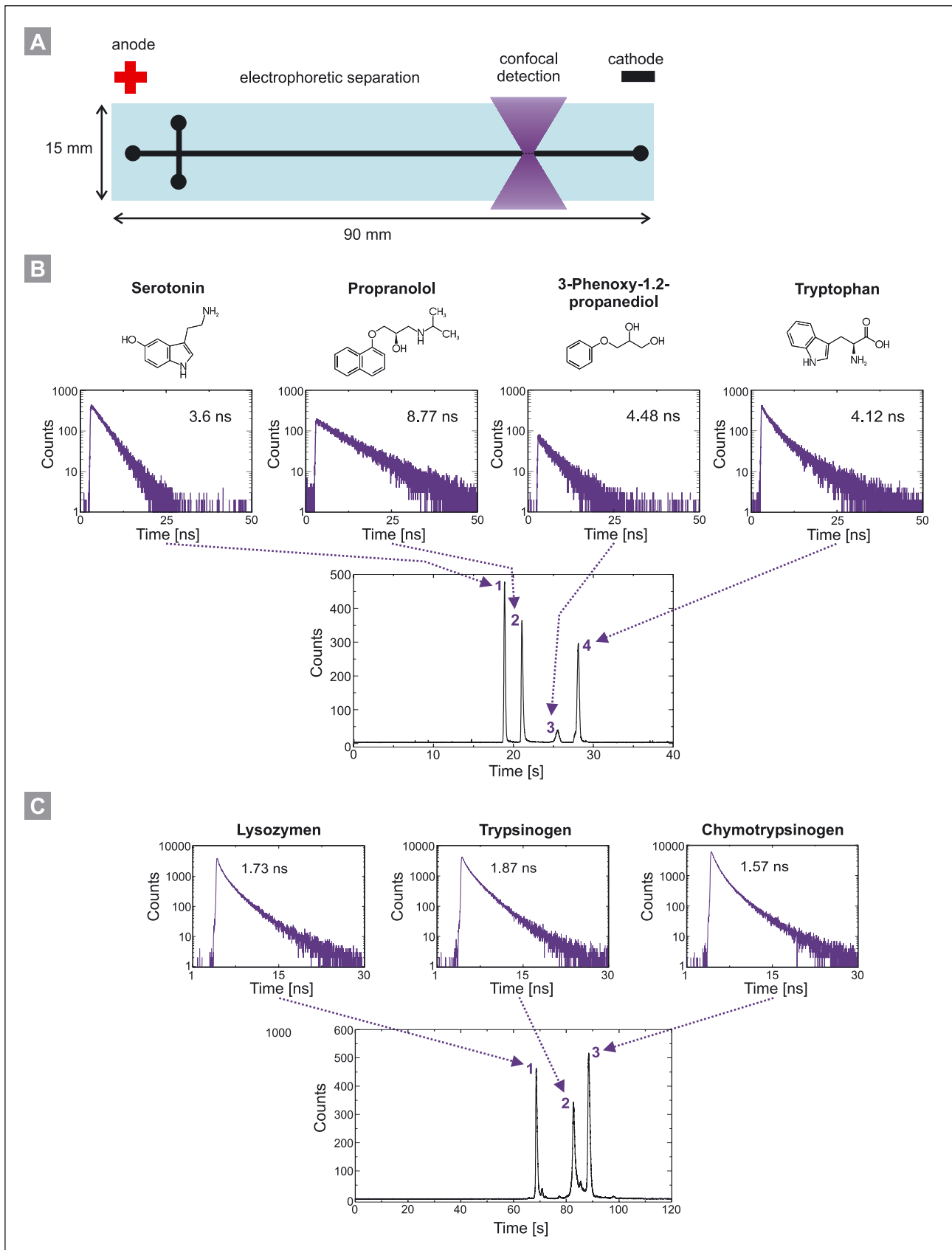
Figure 6: Microchip electrophoretic separation and label-free identification of native analytes. (A) Fused silica microchips with cross injector layout were used. The microchannels were 20 µm in depth and 50 µm in width at the top and mounted within a homemade low conductivity carrier plate on the x,y-translational stage of the MicroTime 200 microscope. (B) Electrophoretic separation of a mixture of small aromatics. 188 µM serotonin (1), 135 µM propranolol (2), 238 µM 3-phenoxy-1.2-propranediol (3), and 196 µM tryptophan (4). Separation buffer: 5 mM borate, pH 9.2. Effective separation length: 5 cm. (C) Electrophoretic separation of a mixture of proteins. 23.3 µM lysozyme (1), 13.9 µM trypsinogen (2), and 13.0 µM chymotrypsinogen (3). Separation buffer: 40 mM phosphate, pH 3.0. Microfluidic channels were coated with 0.01 % w/v hydroxypropylmethylcellulose. Effective separation length: 4.5 cm. Lifetime acquisition: Excitation at 266 nm with 20 MHz repetition rate and ~10 ps pulses at 5 nJ (Cougar, Time-Bandwidth). Quartz objective, 401x, NA 0.8. Optical filters Z266RDC, bandpass 350/50 and 325/40. Detection with super-bialkali PMT[5].

Table 1: Determined UV lifetime parameters of electrophoretically separated small aromatics and proteins.

Analyte	τ_1 [ns]	τ_2 [ns]	A_1 [%]	τ_{Amp} [ns]	τ_{Int} [ns]
serotonin	3.56	-	100	3.56	3.56
propranolol	8.76	-	100	8.76	8.76
3-phenoxy-1,2-propanediol	2.44	6.46	64.2	3.88	4.84
tryptophan	2.19	6.82	55.0	4.28	5.52
lysozyme	0.90	3.13	79.2	1.37	1.96
trypsinogen	1.18	2.51	43.3	1.76	2.00
chymotrypsinogen	1.20	3.77	89.3	1.47	1.89

Table 2: Number of aromatic amino acids of the analyzed proteins.

Protein	No. amino acids	# Trp	# Tyr	# Phe
trypsinogen (bovine pancreas)	229	4	10	3
α-chymotrypsinogen A (bovine pancreas)	482	16	6	10
lysozyme (chicken egg white)	129	6	2	3

electrophoresis signal. The obtained average lifetimes and standard deviations are listed in Table 1 showing that the compounds could be clearly differentiated.

In addition, microchip electrophoresis combined with fluorescence lifetime measurements were performed with protein mixtures emphasizing the potential for biopolymer analysis. A mixture of 10 µM lysozyme, trypsinogen, and a-chymotrypsinogen were analyzed (Figure 6C). These analytes that contain identical chromophoric groups such as aromatic amino acids show distinct fluorescence lifetimes and multi-exponential fluorescence decays that depend on the ratio of the concerned chromophores and their molecular environment (Table 2). The specific fluorescence lifetimes measured in the deep UV may thus be utilized as an intrinsic molecular marker for microscopic protein discrimination.

Outlook

For the first time we have developed an implementation of deep UV TCSPC in a commercial system. With this novel development, FCS and FLIM are now applicable to a completely new range of fluorophores and enable the detection of naturally occurring dyes in the UV spectrum since the 266 nm laser grants access to the intrinsic fluorescence of tryptophan-containing proteins. Apart from single cells, there is also considerable interest to distinguish the constituents of different tissues for label free-discrimination. While UV light does not penetrate tissue very deep, lifetime based native fluorescence screening finds applications in histology for better tissue differentiation, allowing for discriminating healthy and cancerous cell material, or even for quality control applications as in food science. As the origin of the fluorescence could have multiple molecule sources and might therefore not easily be fitted with a simple exponential approach, the newly developed pattern matching analysis in the SymPhoTime software (PicoQuant) is an essential tool for fast distinction of different tissues. Furthermore, by using the sample scanning mode of the MicroTime 200, the object size is no longer limited by the field of view, thus opening the possibility for in vitro microplate screening even on the large scale.

Due to the open design of the MicroTime 200, the set-up is extendable towards microchip electrophoresis combined with fluorescence lifetime determination which is a powerful technique for specific discrimination of proteins, biomolecules, and other analytes. In combination with deep UV excitation, the system is applicable for label-free on-chip detection and analysis of small aromatics and proteins.

By implementing the TCSPC device TimeHarp 260 into the UV MicroTime 200 set-up, measurements of long-lifetime probes become feasible and at some point make cell as well as tissue studies much easier.

All biological samples display autofluorescence, which is usually the limiting factor in high-sensitivity detection. The autofluorescence usually decays on the nanosecond time scale as do most fluorophores. The usage of long-lifetime probes as lanthanides provides a special tool to overcome this limitation. Lanthanides are uniquely fluorescent metals that display a large Stokes shift, extremely long emission lifetimes of 0.5 to 3 ms and are excitable in the deep UV spectral region. Due to their long decay times, the lanthanides continue to emit even when the autofluorescence already disappeared thus allowing a separation of background vs. probe fluorescence based on the different lifetimes. Furthermore, lanthanides are well-suited for LRET (Luminescence Resonance Energy Transfer). While LRET has been mainly exploited in vitro using Terbium as a LRET donor[6], first steps in the direction of imaging and cell labeling have been performed. The advantages of LRET include insensitivity to light-scattering or background fluorescence artifacts, less uncertainty about the dipole orientation factor, and the ease of selectively measuring energy donor-acceptor distances without having all donors paired with acceptors[7]. Thus, the acceptor decay can be easily analysed, and therefore also small contributions are detectable. Since the TimeHarp 260 permits to study dynamics from picoseconds up to seconds, time-resolved fluorescence and luminescence spectroscopy can be applied in one system.

References and Further Reading

[1] Li, Q., Seeger, S.: Autofluorescence detection in analytical chemistry and biochemistry. S Appl. Spec. Rev., 45, 12-43 (2010)

[2] Schönau, T., Siebert, T., Klemme, D., Haertel, R., Lauritsen, K., Erdmann, R.: Versatile Picosecond Laser Sources for Time-Resolved Fluorescence Microscopy and Diffuse Optical Imaging. Biomedical Optics (BIOMED), Biomed Poster Session II, paper BTu3A.7 (2012)

[3] Lakowicz, J. R.: Principles of Fluorescence Spectroscopy. 3rd edition (2006)

[4] Beyreiss R., Ohla S., Nagl S., Belder D.: Label-free analysis in chip electrophoresis applying deep UV fluorescence lifetime detection. Electrophoresis, Vol. 32, 3108-3114 (2011)

[5] Ohla S., Beyreiss R.,Fritzsche S., Glaser P., Nagl S., Stockhausen K., SchneiderC., Belder D.: Monitoring on-chip pictet-spengler reactions by integrated analytical separation and label-free time-resolved fluorescence. Chemistry – A European Journal, Vol.18, p.1240-1246 (2012)

[6] Yuan F., Griffin L., Phelps L. J., Buschmann V., Weston K., Greenbaum N. L.: Use of a novel Förster resonance energy transfer method to identify locations of site-bound metal ions in the U2-U6 snRNA complex. Nucleic Acids Research, Vol. 35, 2833-2845 (2007)

[7] González, D., Lokhande, N., Vadde, S., Zhao, Q., Cassill, A., Renthal, R.: Luminescence Resonance Energy Transfer in the Cytoplasm of Live Escherichia coli Cells. Biochemistry, 50 (32), 6789-6796 (2011)